Parcellation-induced Variation of Empirical and Simulated Functional Brain Connectivity

Justin Domhof[1,2], Kyesam Jung[1,2], Simon Eickhoff[1,2], Oleksandr Popovych[1,2]

[1]Institute of Neuroscience and Medicine, Brain and Behaviour (INM-7), Research Centre Jülich

[2]Institute for Systems Neuroscience, Medical Faculty, Heinrich-Heine University Düsseldorf

Study motivation

- Dynamical, whole-brain models aim to tie structural (SC) and functional connectivity (FC) together
- How the brain atlas or parcellation influence the modelling results is unkown
- We show a profound influence of the parcellation on the goodness-of-fit
- Graph-theoretical properties of the empirical connectomes explained the group-averaged, but not subject-specific variations

Materials and methods

- Empirical SC and FC derived for 19 atlases and 200 subjects from the HCP[1,2]
- Two types of dynamical whole-brain models (networks of phase oscillators and neural mass models) derived on the basis of the resulting SC
- The models were simulated for each combination of subject and parcellation individually for a wide variety of (global) parameter settings
- Simulated FC matrices were constructed from the simulated time series and correlated with the empirical FC
- Graph-theoretical statistics were extracted from all types of connectivity

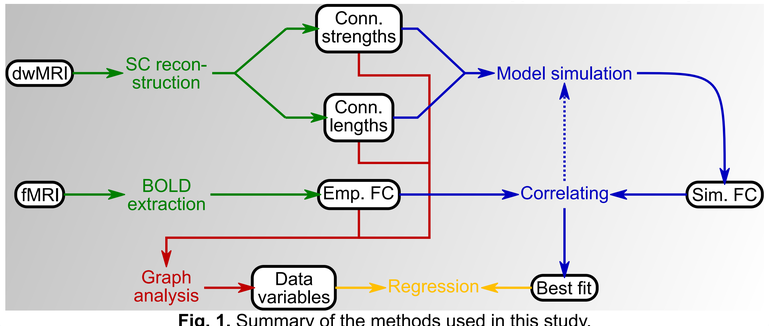

Fig. 1. Summary of the methods used in this study.

Atlases

[1-4] MIST with 31 (1), 56 (2), 103 (3) and 167 (4) parcels[3]
[5-8] Craddock with 38 (5), 56 (6), 108 (7) and 160 (8) parcels[4]
[9-10] Shen with 79 (9) and 156 (10) parcels[5]
[11-12] Schaefer with 100 (11) and 200 (12) parcels[6]
[13-14] Harvard-Oxford with 48 (13) and 96 (14) parcels[7-10]
[15] Desikan-Killiany with 70 parcels[7] -- **[16]** von Economo-Koskinas with 86 parcels[11,12] -- **[17]** AAL (version 2) with 92 parcels[13,14] -- **[18]** Destrieux with 150 parcels[15] -- **[19]** Brainnetome with 210 parcels[16]

1. Van Essen et al. NeuroImage. 2012, 62(4), 2222-2231
2. Van Essen et al. NeuroImage. 2013, 80, 62-79
3. Urchs et al. MNI Open Res. 2019, 1, 3
4. Craddock et al. Human Brain Mapping. 2012, 33(8), 1914-1928
5. Shen et al. NeuroImage. 2013, 82, 403-415
6. Schaefer et al. Cereb Cortex. 2018, 28(9), 3095-3114
7. Desikan et al. NeuroImage. 2006, 31(3), 968-980
8. Frazier et al. AJP. 2005, 162(7), 1256-1265
9. Goldstein et al. Biological Psychiatry. 2007, 61(8), 935-945
10. Makris et al. Schizophrenia Research. 2006, 83(2), 155-171
11. von Economo & Koskinas. Die Cytoarchitektonik Der Hirnrinde Des Erwachsenen Menschen. Springer; 1925
12. Scholtens et al. NeuroImage. 2018, 170, 249-256
13. Rolls et al. NeuroImage. 2015, 122, 1-5
14. Tzourio-Mazoyer et al. NeuroImage. 2002, 15(1), 273-289
15. Destrieux et al. NeuroImage. 2010, 53(1), 1-15
16. Fan et al. Cereb Cortex. 2016, 26(8),

Varying brain parcellation

The goodness-of-fit was influenced highly and independently of the model by the variation of the atlas

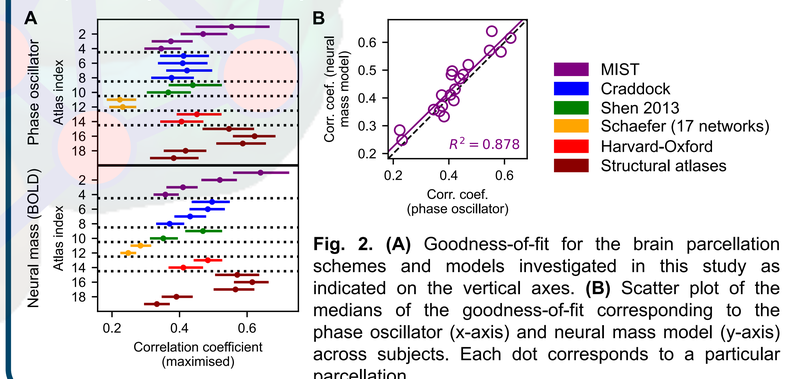

Fig. 2. (A) Goodness-of-fit for the brain parcellation schemes and models investigated in this study as indicated on the vertical axes. **(B)** Scatter plot of the medians of the goodness-of-fit corresponding to the phase oscillator (x-axis) and neural mass model (y-axis) across subjects. Each dot corresponds to a particular parcellation.

Explanation group differences

- PCA applied to the dataset with the median graph-theoretical statistics across subjects for all parcellations
- PC scores related to goodness-of-fits via linear regression
- Only 2 PCs explain up to 80% of variance in the goodness-of-fit

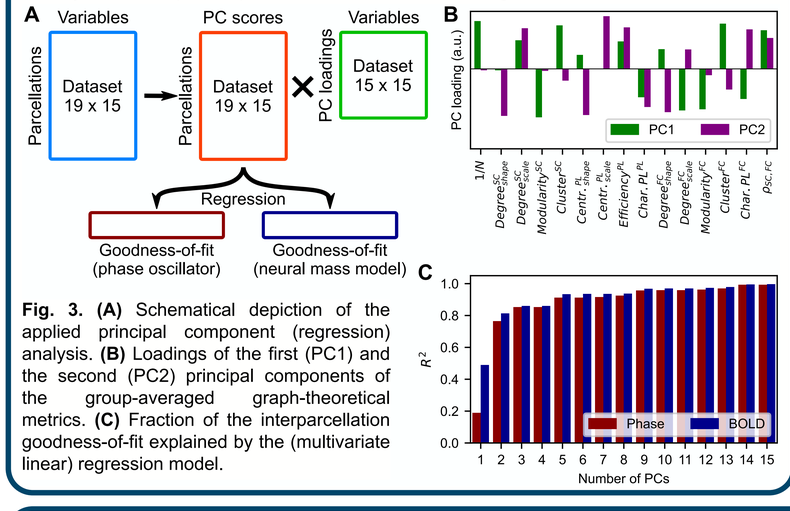

Fig. 3. (A) Schematical depiction of the applied principal component (regression) analysis. **(B)** Loadings of the first (PC1) and the second (PC2) principal components of the group-averaged graph-theoretical metrics. **(C)** Fraction of the interparcellation goodness-of-fit explained by the (multivariate linear) regression model.

Simulated network properties

- Graph measures of empirical FC and simulated FC providing best fit were related
- However they agreed with each other to different extents for the two considered models

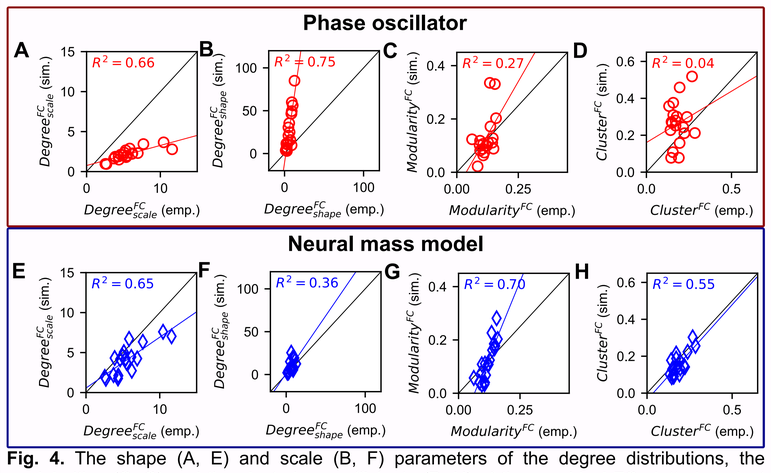

Fig. 4. The shape (A, E) and scale (B, F) parameters of the degree distributions, the modularities (C, G) and the clustering coefficients (D, H) of the empirical FC plotted against those of the simulated FC that best fitted the empirical one and is generated by the phase oscillator (A-D) and neural mass model (E-H). Symbols, coloured and black lines stand for individual parcellations, regression lines and the diagonal x=y, respectively.

Explaining subject variance

(Linear) regressions of the graph measures with the goodness-of-fits of individuals yield low amounts of explained variances that vary considerably across parcellations.

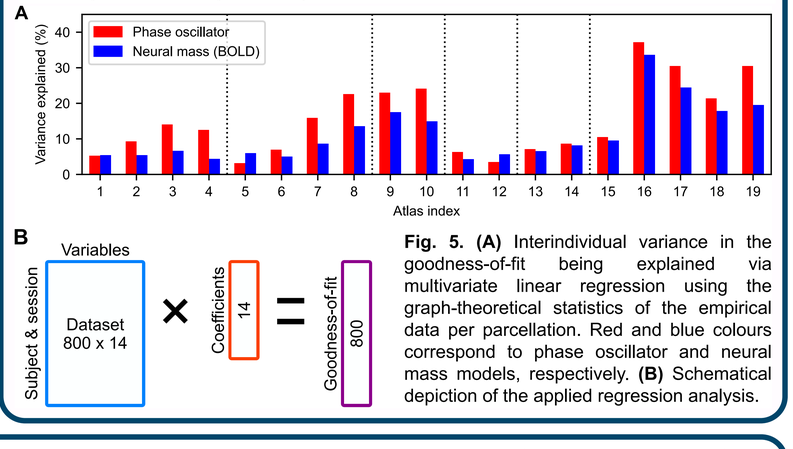

Fig. 5. (A) Interindividual variance in the goodness-of-fit being explained via multivariate linear regression using the graph-theoretical statistics of the empirical data per parcellation. Red and blue colours correspond to phase oscillator and neural mass models, respectively. **(B)** Schematical depiction of the applied regression analysis.

This study was made possible through funding from the Helmholtz Association and the European Union's Horizon 2020 Research and Innovation Program (grant agreements 785907 (HBP SGA2), 945539 (HBP SGA3) and 826421 (VirtualBrainCloud)). Also, the authors gratefully acknowledge the computing time granted through JARA on the supercomputer JURECA at Forschungszentrum Jülich.